Compound screening in primary human airway basal cells identifies Wnt pathway activators as potential pro-regenerative therapies

Yuki Ishii[1†], Jessica C. Orr[1,2†], Marie-Belle El Mdawar[1], Denise R. Bairros de Pilger[3], David R. Pearce[4], Kyren A. Lazarus[1], Rebecca E. Graham[5,6], Marko Z. Nikolić[1], Robin Ketteler[3], Neil O. Carragher[5,6], Sam M. Janes[1*] and Robert E. Hynds[2,4*]

1) Lungs for Living Research Centre, UCL Respiratory, University College London, London, U.K.
2) Epithelial Cell Biology in ENT Research Group, Developmental Biology and Cancer Department, UCL Great Ormond Street Institute of Child Health, University College London, London, U.K.
3) MRC Laboratory for Molecular Cell Biology, University College London, London, U.K.
4) UCL Cancer Institute, University College London, London, U.K.
5) Edinburgh Cancer Research, Institute of Genetics and Cancer, University of Edinburgh, Western General Hospital, Edinburgh, U.K.
6) Cancer Research UK Scotland Centre, U.K.

[†] These authors contributed equally.

* Correspondence:
Robert E. Hynds (rob.hynds@ucl.ac.uk)
Sam M. Janes (s.janes@ucl.ac.uk)

Running title: Wnt activation in airway basal cells

Keywords: lung regeneration, epithelium, cell proliferation, compound screening, respiratory biology

Summary statement: Ishii, Orr and colleagues perform a high-throughput screen of 1,429 compounds in primary human airway epithelial cells, identifying Wnt activating compounds as promoters of proliferation.

ABSTRACT

Regeneration of the airway epithelium restores barrier function and mucociliary clearance following lung injury and infection. Basal cells are tissue-resident airway stem cells that enact regeneration, yet the mechanisms regulating their proliferation and differentiation remain incompletely understood. To identify compounds that promote primary human airway basal cell proliferation, we performed phenotype-based compound screening of 1,429 compounds (from the ENZO and Prestwick Chemical libraries) in 384-well format using primary cells transduced with lentiviral luciferase. 16 pro-proliferative compounds validated in independent donor cell cultures, with several hit compounds activating the Wnt signalling pathway. The effects of compounds on proliferation were further explored in concentration-response, colony formation and 3D organoid assays. Structurally and functionally-related compounds that more potently induced both Wnt activation and basal cell proliferation were investigated. One such compound, 1-azakenpaullone, induced Wnt target gene activation and basal cell proliferation in mice in the absence of tracheal injury. Our results demonstrate the pro-proliferative effect of small-molecule Wnt activators on airway basal cells. These findings contribute to the rationale to develop novel approaches to modulate Wnt signalling during airway epithelial repair.

INTRODUCTION

Human airways are lined by a pseudostratified epithelium that acts as a physical barrier and enacts mucociliary clearance to remove inhaled particles and pathogens from the lungs (Bustamante-Marin and Ostrowski, 2017). Maintaining these functions during homeostasis and following injury is essential for lung health. Tissue-resident basal stem cells can self-renew and differentiate to replenish airway epithelial cell lineages (Basil et al., 2020; Rock et al., 2009).

Airway epithelial repair is a feature of a range of respiratory conditions. Influenza infection leads to tracheobronchitis and cytonecrosis, with desquamation of epithelial cells into the luminal space (Taubenberger and Morens, 2008; Walsh et al., 1961). Sloughing of the airway epithelium is also a feature of respiratory syncytial virus (RSV) (Johnson et al., 2007) or rhinovirus infections (Turner et al., 1982). In chronic lung disease, basal cell stress and loss of progenitor function have been proposed as mechanisms underlying chronic obstructive pulmonary disease (Ghosh et al., 2018; Staudt et al., 2014; Wijk et al., 2021). Additionally, basal cells from asthma patients exhibit functional defects *in vitro* (Kicic et al., 2010; Stevens et al., 2008). Dysregulated airway repair can also lead to chronic airway inflammation and fibrosis in epidermolysis bullosa (Lau et al., 2024), and bronchiolitis obliterans-like pathologies in experimental models (O'Koren et al., 2013). Promoting airway epithelial regeneration is also a key aim of future lung regenerative medicine approaches, including tissue transplantation approaches where promotion of the endogenous epithelial infiltration of the graft is desirable, and following airway epithelial cell transplantation. As such, understanding the mechanisms regulating basal cell function and developing approaches to modulate basal cell behaviour are of significant interest (Hynds, 2022).

Drug development is a costly process, with many candidate drugs failing due to a lack of efficacy or toxicity concerns in on- and off-target effects (Sun et al., 2022). Since it takes, on average, 10-15 years before a new medicine can reach patients (Berdigaliyev and Aljofan, 2020), drug repurposing (i.e. identifying new uses for approved medications outside the scope of the original indication) is an attractive approach (Ashburn and Thor, 2004). Molecules that have been found to be safe in preclinical models and clinical trials in another setting increases the chance of success and can reduce the time and investment required to take therapies from the bench to the bedside (Pushpakom et al., 2019).

Airway regeneration can be modelled in primary cell cultures. Human bronchial epithelial cells (HBECs) proliferate in both 2D or 3D culture systems (Hiemstra et al., 2018; Nizamoglu et al., 2023; Orr and Hynds, 2021), and can be induced to differentiate in air-liquid interface (ALI) (Fulcher et al., 2005) or organoid cultures (Danahay et al., 2015). In recent years, the adaptation of cell culture models to 96-, 384- or 1536- format plates have allowed for higher throuput phenotypic screening (Bloom, 2021; Mayr and Bojanic, 2009). Here, we combine primary airway basal cell culture with compound screening to identify novel modulators of airway basal cell proliferation. Compounds that were identified as promoting basal cell proliferation were further validated in both 2D and 3D cell culture models to assess their effects on basal cell proliferation and differentiation.

RESULTS AND DISCUSSION

Compound screening in primary airway basal cells

Primary human bronchial epithelial cell cultures were established from endobronchial biopsy specimens. Cells underwent lentiviral transduction with a pHIV-Luc-zsGreen construct and fluorescence activated cell sorting to purify zsGreen-positive cells (**Fig. S1A-C**). This enabled 384-well format screening for modulators of basal cell proliferation by monitoring bioluminescence following the addition of luciferin to the culture medium (**Fig. 1A**). In validation experiments, bioluminescence signals correlated strongly with Hoescht 33342 nuclei counts (**Fig. 1B** and **Fig. S1D**) suggesting that our screening approach successfully reports cell proliferation. As a positive control, we tested Y-27632, a small-molecule inhibitor that is known to induce basal cell proliferation (Horani et al., 2013; Reynolds et al., 2016). As expected, the bioluminescence signal increased following the addition of Y-27632 (**Fig. 1C**). Calculation of the signal window (10.09) and Z' factor (0.7) between control and Y-27632-treated wells indicated a robust assay window (signal window ≥ 2, Z' factor ≥ 0.4; Iversen et al., 2012). The hit threshold was set at 1.96 standard deviations above the plate mean (i.e. a mean Z score above 1.96).

We screened a total of 1,429 compounds from the ENZO chemical library (of epigenetic modulator and proteinase and kinase inhibitors) and the Prestwick Chemical library (of compounds that are approved for clinical use by the FDA, EMA and other agencies and have been selected to represent broad pharmacological diversity). We identified 27 compounds (**Table S1**) that increased luciferase activity above the threshold value (**Fig. 1D/1E**), including Y-27632. An additional 61 compounds significantly reduced the number of basal cells (**Fig. 1D**), likely including compounds that inhibit essential processes, inhibit the cell cycle or are toxic to basal cells. Z scores for all compounds tested can be found in **Table S2**. The establishment of a robust airway basal cell proliferation screening protocol further demonstrates the ability to perform screening in primary airway epithelial cells. Our approach adds to previous 96-well format screens for modulators of ciliogenesis in mouse organoids from transgenic mice (Tadokoro et al., 2014), readthrough agents in primary ciliary dyskinesia air-liquid interface cultures (Lee et al., 2021) and anti-viral compounds in healthy air-liquid interface cultures (Sen et al., 2024), as well as a 384-well plate screen for inhibitors of thymic stromal lymphopoietin (TSLP) production performed in commercially available airway basal cells (Orellana et al., 2018).

To validate that hit compounds accelerate basal cell proliferation, we re-ordered them from independent suppliers and performed concentration-response proliferation assays at the same timepoint. In primary human bronchial epithelial cell cultures that had undergone lentiviral transduction with pHIV-Luc-zsGreen (n = 3 donors), 17 hit compounds (10 from the ENZO chemical library and 7 from the Prestwick Chemical library) increased luciferase activity, including Y-27632 (**Fig. 2A, Fig. S2A**). Five of six hit compounds tested from the Prestwick Chemical library in organoids (or 'bronchospheres') led to an increase in organoid size (**Fig. S2B**).

Overall, this screen suggests multiple avenues for future research, including suggesting compounds with re-purposing potential in lung regeneration applications.

Wnt pathway-activating molecules promote airway basal cell proliferation

Four validated hit compounds - indirubin-3'-monoxime, kenpaullone, nabumetone and phenazopyridine - have been previously reported to activate canonical Wnt signalling. Wnt signalling is involved in the specification of lung progenitor cells (Goss et al., 2009) and the proximal-distal patterning of airways during development (Hashimoto et al., 2012; Shu et al., 2005), and influences post-natal airway epithelial cell proliferation (Aros et al., 2020a; Hsu et al., 2014; Ievlev et al., 2022; Lynch et al., 2016), differentiation (Cooney et al., 2023; Haas et al., 2019; Malleske et al., 2018; Schmid et al., 2017) and the formation of ageing-associated glandular-like epithelial invaginations (Aros et al., 2020b). As such, we further investigated the effects of these compounds in colony formation assays finding that kenpaullone and phenazopyridine increased colony forming efficiency (**Fig. 2B**). We also tested the effects of the ENZO library hit compounds on untransduced primary human bronchial epithelial cells and found that kenpaullone was the compound that most potently induced basal cell proliferation, followed by indirubin-3'-monoxime, apigenin and PD-98059 (**Fig. S3**). In 3D organoids, the addition of kenpaullone and indirubin-3'-monoxime significantly increased organoid size (**Fig. 2C**). At concentrations of these compounds that increased organoid size, the differentiation potential of basal cells was preserved, with both acetylated tubulin (ACT) and mucin-5AC (MUC5AC) observed by immunofluorescence (**Fig. 2D**), indicative of multiciliated and mucosecretory cell differentiation, respectively.

A previous screening study identified potential lung pro-regenerative therapies by examining the extent to which compounds in the Prestwick Chemical library activated a TCF/LEF reporter in 3T3 mouse embryonic fibroblasts (Costa et al., 2021). Two of the five candidate drugs identified in that study, phenazopyridine and nabumetone, increased basal cell

proliferation in both screening (**Fig. 1E**) and validation experiments (**Fig. 2A**). Consistent with our human cell data, the previous study found that phenazopyridine increased the number of mouse lung organoids in cell culture.

Kenpaullone was the most potent pro-proliferative compound identified from the ENZO library screen (**Fig. 2A**) and, of the four reported Wnt activating molecules identified in our screen, induced the highest firefly luciferase activity in HBEC3-KT cells transfected with TOPFlash plasmids (in which firefly luciferase expression is controlled by a minimal promoter and multiple TCF binding sites; **Fig. 3A**). Since more potent and selective derivatives were available for two of the Wnt-activating screening hits identified (kenpaullone and indirubin-3'-monoxime), we compared the effect of kenpaullone to 1-azakenpaullone (Kunick et al., 2004) and 6-bromoindirubin-3-oxime (BIO) (Meijer et al., 2003). Basal cells continued to express the transcription factor TP63, a protein associated with basal cell stem cell potential (Warner et al., 2013), after culture in all three compounds (**Fig. S4A**), and both 1-azakenpaullone and BIO induced higher TOPFlash expression in HBEC3-KT cells than kenpaullone, signifying increased Wnt signalling induction (**Fig. 3B**). This conclusion was further supported by the finding that pretreatment with iCRT14, a small-molecule inhibitor that blocks the transcriptional activity of β-catenin, prevented TOPFlash activation in BIO-treated cells (**Fig. 3B**). We observed higher expression of the Wnt target genes *LEF1* and *AXIN2* in BIO-treated cells (**Fig. 3C**). The expression of *CCND1* and *MYC* were unchanged in kenpaullone, 1-azakenpaullone and BIO treated cells (**Fig. S4B**). All three compounds increased basal cell proliferation as measured by the CellTiter-Glo luciferase assay performed on non-transduced primary airway basal cells (**Fig. 3D**). Moveover, pre-treatment with iCRT14 prevented the increases in proliferation seen with addition of kenpaullone, 1-azakenpaullone or BIO (**Fig. 3E**). Since kenpaullone acts as an inhibitor of both glycogen synthase kinase 3 beta (GSK3β) and cyclin-dependent kinase (Leost et al., 2000; Zaharevitz et al., 1999), this iCRT14 sensitivity suggests that the mechanism of action is canonical Wnt pathway activation. Finally, the compounds increased organoid size in 3D culture in a concentration-dependent manner (**Fig. 3F**). Organoids cultured in medium containing all three compounds displayed both ACT+ ciliated cells and MUC5AC+ mucosecretory cells (**Fig. 3G**) indicating their retained ability to undergo airway differentiation in the presence of these compounds.

1-Azakenpaullone activates Wnt signalling in mouse trachea and lung in vivo

Since 1-azakenpaullone had previously been administered *in vivo* in mice (Feng et al., 2012), we performed an initial assessment of the potential of 1-azakenpaullone to modulate

airway basal cell Wnt activation and proliferation *in vivo*. We administered 1-azakenpaullone (3 mg/kg) or PBS along with EdU intraperitoneally in C57Bl/6 mice (**Fig. 4A**). 24 hours following administration, we found increased proliferation as judged by EdU positivity within the epithelium (**Fig. 4B**). We also found trends towards increased expression of the Wnt target genes *Myc* and *Ccnd1* in tracheal cells, and a significant increase in *Myc*, but not *Ccnd1* in lung tissue from the same mice (**Fig. 4C**). No changes were observed in *Axin2* or *Lef1* expression in either tissue (**Fig. S4C**). This was supported by increased protein expression of c-Myc and cyclin D1 in 1-azakenpaullone-treated mouse lung tissue (**Fig. 4D**).

Overall, this study confirms canonical Wnt pathway activation as a pro-proliferative signal in airway epithelial cells cultures and our *in vivo* study demonstrates Wnt activation within the trachea and lung following 1-azakenpaullone administration to uninjured mice. Given that there are 19 Wnt ligands in humans (Rim et al., 2022), Wnt signalling regulation during airway regeneration is likely to be complex, as well as spatiotemporally controlled. The source of Wnt signals *in vivo* seems to differ between airway regeneration (stromal-derived) and homeostasis (airway epithelium-derived) (Aros et al., 2020b)**.** Additionally, non-canonical (β-catenin-independent) Wnt signalling can counteract the canonical pathway to inhibit regeneration in alveolar tissue (Baarsma et al., 2017). Future considerations for manipulating the Wnt pathway to improve airway regeneration should account for potential differences in the effect of pathway activation during injury and homeostasis, as previous studies demonstrate that Wnt signalling acts to maintain ΔNp63-expressing stem cells during homeostasis (Haas et al., 2019), with high signalling levels leading to basal cell hyperplasia that is reversible by Wnt inhibition (Aros et al., 2020a). Indeed, constitutive activation of β-catenin during development impacts epithelial cell morphogenesis and leads to polyp formation (Li et al., 2009), persistent Wnt signalling leads to squamous differentiation of airway basal cells (Zhang et al., 2023), and human airway premalignant lesions and squamous cell carcinomas show evidence of Wnt activation (Aros et al., 2020a).

MATERIALS AND METHODS

Cell culture

Patient tissue was obtained from regions of histologically normal airway via endobronchial biopsy or as segments of normal lung following lobectomy procedures with informed patient consent. Ethical approval was obtained through the National Research Ethics Committee (REC reference 18/SC/0514). Cell culture plates and flasks were Nunc branded and purchased from Thermo Fisher Scientific. Cells were cultured at 5% CO_2, 21% O_2 at 37°C.

3T3-J2 mouse embryonic fibroblasts (a gift from Prof Fiona Watt, King's College London, U.K.) were cultured in Dulbecco's Modified Eagle Medium (DMEM; Gibco, 41966) with 9% bovine serum (26170043, Gibco) and 1x penicillin/streptomycin. Feeder layers were generated between passages 9-12. Cells were mitotically inactivated by treatment with 4 µg/mL mitomycin C (M4287, Sigma-Aldrich) in cell culture medium for three hours. Cells were trypsinized and plated at 20,000-30,000 cells/cm^2. Epithelial cells were added the following day.

Endobronchial biopsies and lobectomy tissue (**Table 1**) arrived in the laboratory on ice in transport medium (αMEM (22561, Gibco) supplemented with 1x penicillin/streptomycin (15140-122, Gibco), 10 µg/mL gentamicin (15710-049, Gibco), and 250 ng/mL amphotericin B (BP264550, Fisher Bioreagents).

To generate single cell suspensions, biopsies and airway tissue were incubated in 16 U dispase (354235, Corning) in RPMI (21875, Gibco) for 20 minutes at room temperature and then mechanically disrupted using sterile forceps. This was followed by incubation in 0.1% trypsin/EDTA (59418C, Sigma-Aldrich) for 30 minutes at 37°C. Both dispase and trypsin/EDTA incubations were neutralised with FBS. The digested tissues were filtered through a 100 µm cell strainer (352360, Falcon). Single cell suspensions were centrifuged at 300 x g for 5 minutes and resuspended in relevant media for counting and plating.

Donor ID	Type	Location	Self-reported Ethnicity	Age at collection (yrs)	Sex	Smoking status	Respiratory comorbidities recorded
1	Bronchial	lingula	White	73	M	Former	No
2a	Bronchial	RUL	White	77	M	Former	Dysplasia and emphysema
2b	Bronchial	RML	White	80	M	Former	Dysplasia and emphysema
3	Bronchial	LLL	White	71	M	Current	No
4	Bronchial	LLL	Black African	61	M	Never	Asthma
5	Bronchial	LUL/LLL carina	White	67	M	Current	No
6	Bronchial	LUL	White	58	F	Current	Previous Squamous cell cancer
7	Bronchial	Unknown	White	63	M	Never	No
8	Bronchial	Unknown	Black African	60	M	Current	No
9	Lobectomy	RUL	White	76	M	Former	COPD and lung emphysema
10	Lobectomy	LLL	White	78	F	Former	Previous small cell cancer
11	Lobectomy	LLL	White	73	F	Former	No
12	Bronchial	RUL	White	73	M	Current	No

Table 1: Donor information for primary human airway basal cell cultures.

Epithelial cell culture medium (Butler et al., 2016; Hynds et al., 2019; Liu et al., 2012) consisted of a 3:1 ratio of DMEM supplemented with 9% foetal bovine serum (FBS) (10270106, Gibco) and 1x penicillin/streptomycin with Ham's F12 (21765, Gibco); supplemented with 5 µM Y-27632 (T1725, Tebu-Bio), 25 ng/mL hydrocortisone (H0888, Sigma-Aldrich), 0.125 ng/mL epidermal growth factor (EGF; PHG0315, Gibco), 5 µg/mL insulin (I5500, Sigma-Aldrich), 0.1 nM cholera toxin (C8052, Sigma-Aldrich), 250 ng/mL amphotericin B (BP2645, Fisher Bioreagents), 10 µg/mL gentamicin.

FAD medium consisted of DMEM/Ham's F12 in a 3:1 ratio supplemented with 10% FBS, 1x penicillin/streptomycin, 1% adenine (A3159, Sigma-Aldrich), 0.5 µg/mL hydrocortisone, 10 ng/mL EGF, 5 µg/mL insulin, 0.1 nM cholera toxin, 2×10^{-5} T3 (T5516, Sigma-Aldrich), 10 µg/mL gentamicin and 250 ng/mL amphotericin B.

The differential trypsin sensitivity of 3T3-J2 fibroblasts and epithelial cells was used to isolate epithelial cell populations from co-cultures. Co-cultures were washed with phosphate-buffered saline (PBS; D8537, Sigma-Aldrich) and 0.05% trypsin/EDTA (25300054, Gibco) was added for two minutes to remove the 3T3-J2 fibroblasts, which are more sensitive to trypsin than the strongly adherent epithelial cells. Flasks were then washed with PBS and 0.05% trypsin/EDTA was added a second time for 5-10 minutes to detach the epithelial cells. Cells were centrifuged at 300 x g for five minutes and resuspended in the required media for counting and plating.

The HBEC3-KT cell line (CRL-4051, ATCC) was cultured in Airway Epithelial Cell Basal Medium (PCS-300-030, ATCC) supplemented with the Bronchial Epithelial Cell Growth Kit (PCS-300-040, ATCC) or in Keratinocyte SFM (17005-042, Thermo Fisher Scientific), a serum-free medium supplemented with recombinant EGF and bovine pituitary extract. Cells were passaged by trypsinization with 0.05% trypsin/EDTA. Cells were centrifuged at 300 x g for five minutes to ensure trypsin removal.

Cells cultured in epithelial cell culture medium were cryopreserved in 50% cell culture medium, 42.5% ProFreeze (BP12-769E, Lonza) and 7.5% DMSO. Cells cultured in FAD medium were frozen in 1x Cell Freezing Medium-Glycerol (C6039, Merck). Cryovials were transferred to a CoolCell and placed in an -80°C freezer to cool by one degree celsius per minute. Cryopreserved cells were then stored at -150°C.

Virus production

HEK293Ts were cultured in DMEM supplemented with 10% FBS and 1x penicillin/streptomycin. Antibiotics were omitted for one passage prior to and during transfection.

Viral supernatants were produced by co-transfecting HEK293T cells at 70-80% confluency in a T175 flask with 20 µg pHIV-Luc-ZsGreen (gift from Bryan Welm (Addgene plasmid #39196; http://n2t.net/addgene:39196; RRID:Addgene_39196)), 13 µg pCMVR8.74 (gift from Didier Trono (Addgene plasmid #22036; http://n2t.net/addgene:22036; RRID:Addgene_22036)) and 7 µg pMD2.G (gift from Didier Trono (Addgene plasmid #12259; http://n2t.net/addgene:12259; RRID:Addgene_12259)) using JetPEI (101000053, Polyplus Transfection) and following the manufacturer's protocol. Viral supernatants were collected 48 hours and 72 hours post-transfection and filtered through a 0.45 µm filter (6780-2504, Whatman). Supernatant was combined with PEGit concentrator (5X) (LV810A-1, System Biosciences) overnight at 4°C and centrifuged at 1500 x g for 45 minutes at 4°C. The supernatant was removed, and the viral pellet was resuspended in 1/10th of the original supernatant volume in DMEM supplemented with 25 mM HEPES. Concentrated supernatants were stored at -80°C until use.

Lentiviral transduction of primary airway basal cells

Epithelial cells were plated at 150,000 cells per well in a 6-well plate on 3T3-J2 feeder layers. The following day, cells were transduced with the addition of 100 µL concentrated virus and polybrene (4 µg/mL; Santa Cruz) to the cell culture medium. Medium was replaced 7 hours after the addition of the virus.

Transduced cells were enriched by fluorescence-activated cell sorting (FACS) using their expression of zsGreen. Single cell suspensions of epithelial cells were collected by differential trypsinization and were filtered through a 70 µm strainer (352350, Falcon), centrifuged 300 x g for five minutes, and resuspended in FACS buffer (PBS, 1% FBS, 25 mM HEPES and 1 mM EDTA). FACS experiments were performed using either a BD FACS Aria or a BD FACS Aria Fusion sorter.

Compound screening in primary airway basal cells

1,429 compounds from the ENZO library (159 compounds) and the Prestwick Chemical library (1277 compounds) were tested. 7 compounds were shared between both libraries, giving a total of 1,429 unique compounds in our study. Compounds were pre-plated in a 384-well format at 2 mM in DMSO. The plates were stored in a nitrogen-purged StoragePod

(Roylan Developments) in 5% humidity with 5% O_2. Potential hit compounds were re-ordered for validation experiments. Compounds (**Table S3**) were reconstituted as 10 mM stocks in DMSO, aliquoted and stored at - 20°C to avoid multiple freeze-thaw cycles.

Primary airway basal cells transduced with the pHIV-Luc-ZsGreen construct were expanded in epithelial cell culture medium and cultured for one passage in FAD medium (without Y-27632) prior to plating in 384-well plates (142761, Thermo Fisher Scientific). Compound libraries and DMSO were added to the assay plate using an ECHO 550 liquid handler (Labcyte). Cells were seeded at 2,000 cells/well in FAD medium using a plate dispenser under sterile conditions. After four days of culture, medium was removed, and luciferin was added to cells at 150 µg/mL in FAD medium using the plate dispenser. After ten minutes, bioluminescence was measured using a Envision II plate reader (PerkinElmer). Relative light units were normalised to the DMSO control well values. Data analysis was performed in R. For nuclei visualisation medium was removed and 2 µg/mL Hoechst 33342 (H3570, Invitrogen) in FAD medium was added. After ten minutes the wells were imaged and nuclei counted using a Cytation 3 imaging reader (Biotek).

Cell proliferation experiments

For experiments in non-transduced HBECs, primary airway basal cells were expanded on 3T3-J2 feeder cells in FAD medium. For proliferation assays, HBECs (without feeder cells) were seeded at 2,000 cells/well in 384-well plates using a E1-ClipTip multichannel pipette (Thermo Fisher Scientific) and compounds were added at the time of seeding. After six days in culture, cells were lysed using CellTiter-Glo (G7570, Promega) reagents, according to the manufacturer's protocol. Bioluminescence was measured using a Envision II plate reader.

To investigate the effect of inhibiting canonical Wnt activation, primary airway basal cells that had been cultured in FAD medium prior to the assay were seeded at 2,000 cells/well in a 384-well plate in FAD medium containing 10 µM inhibitor of β-catenin responsive transcription 14 (iCRT14; HY-16665, MedChemExpress). The following day hit compounds were added to the wells. After six days in culture, the cell viability was measured using the CellTiter-Glo protocol; the relative light unit was measured by a Envision II plate reader.

TOPFlash assay

The HBEC3-KT cell line was seeded in 6-well plates at 900,000 cells/well. The following day cells were co-transfected with the M50 Super 8x TOPFlash (a gift from Randall Moon, Addgene plasmid #12456; http://n2t.net/addgene:12456; RRID:Addgene_12456), the M51 Super 8x FOPFlash – an inactive TOPFlash mutant (a gift from Randall Moon, Addgene

plasmid #12457) and the pRL SV40 construct (E2231, Promega) using jetOPTIMUS (101000051, Polyplus) according to the manufacturer's instructions. Medium was changed after 6 hours. The next day, cells were seeded at 20,000 cells/well in a 384-well plate and compounds were added after three hours. Luciferase activity was measured using Dual-Glo luciferase assay system by a Envision II plate reader (PerkinElmer) 48 hours after compound addition.

Colony formation assays

To calculate colony forming efficiency, primary airway basal cells were seeded at 1,000 cells/well on 6-well plates that had been pre-coated with collagen I and 3T3-J2 feeder cells (Hynds et al., 2018). Experimental compounds or an equivalent DMSO volume for control wells were added the following day. Medium was changed twice per week. On day 10, cells were fixed in 4% PFA for 20 minutes and stained with crystal violet solution (HT90132, Sigma-Aldrich) for 15 minutes at room temperature. Plates were washed thoroughly with water and dried overnight. Plates were scanned using an Epson Perfection V700 PHOTO Scanner. Colonies were manually counted using a brightfield microscope. Colonies were defined as contiguous groups of more than ten cells. Colony forming efficiency (%) was calculated as (number of colonies counted/number of cells seeded) x 100.

Organoid/bronchosphere culture

Bronchospheres were cultured as per previously published methods (Hynds et al., 2019). Differentiation medium consisted of 50% DMEM and 50% BEBM supplemented with BEGM SingleQuots (except amphotericin B, triiodothyronine, and retinoic acid; CC-3171 and CC-4175, Lonza). Medium was supplemented with 100 nM all-trans retinoic acid (R2625, Sigma-Aldrich) at time of use. Briefly, wells of an ultra-low attachment 96-well plate (3474, Corning) were coated with 30 µL 25% matrigel (354230, Corning) in bronchosphere medium and returned to the incubator at 37°C for 30 minutes. Epithelial cells were seeded at 2,500 cells/well in 65 µL 5% matrigel in bronchosphere medium containing 5 µM Y-27632. Bronchospheres were fed with 50 µL bronchosphere medium supplemented with experimental compounds or equivalent DMSO volume for control wells on days 3, 10 and 17 of culture.

On Day 21, whole well images were taken and image analysis was performed with OrgaQuant (Kassis et al., 2019). Bronchospheres were collected in ice cold PBS and centrifuged at 300 x g for five minutes. Bronchospheres were fixed in 4% PFA on ice for 30 minutes and then centrifuged at 400 x g for five minutes. Bronchospheres were then washed with ice cold PBS and transferred to a well of a V-bottomed 96-well plate. The plate was

centrifuged at 400 x g for 5 minutes and bronchospheres were resuspended in 120 μL pre-warmed HistoGel (HG4000012, Fisher Scientific). After ten minutes on ice, the gel was transferred to 70% ethanol at 4°C before being processed in a Leica TP1050 tissue processor. Samples were embedded in type 6 paraffin wax (8336, Epredia) using an embedding station (Sakura Tissue-TEK TEC) and 5 μm sections were cut on a Microm HM 325 microtome.

Immunohistochemistry, immunofluorescence staining and immunocytochemistry
For immunofluorescence staining of samples on slides, slides were dewaxed using an automated protocol. Slides were washed in PBS and a hydrophobic ring was drawn around the sample using an ImmEdge pen (H-4000, Vector Laboratories). Sections were blocked with 1% bovine serum albumin (BSA; 1.12018.0100, Merck), 5% normal goat serum (NGS; Abcam, ab7481) and 0.1% triton X-100 (X-100, Sigma-Aldrich) in PBS for one hour at room temperature. Primary antibodies raised against TP63 (ab124762, Abcam; 1:300), KRT5 (905901, Biolegend; 1:500), MUC5AC (M5293, Sigma-Aldrich; 1:500) and ACT (T6793, Sigma-Aldrich; 1:500) were diluted in block buffer and applied to slides overnight at 4°C. Slides were washed twice in PBS. For EdU detection the Click-iT™ EdU Cell Proliferation Kit for Imaging, Alexa Fluor™ 488 dye (C10337, Thermo Fisher Scientific) was used according to the manufacturer's protocol prior to secondary antibody application.

Secondary antibodies conjugated to species appropriate Alexa Fluor dyes were diluted 1:1,000 in 5% NGS, 0.1% triton in PBS and applied to slides for three hours at room temperature in the dark. 100 ng/mL DAPI (D9542, Sigma-Aldrich) in PBS was applied to the slides for 20 minutes. Slides were washed twice in PBS and a coverslip was applied manually with Immu-Mount (9990402, Thermo Fisher Scientific). Images were acquired using a Leica DMi8 fluorescence microscope.

For immunocytochemistry, 8-well chamber slides were pre-coated with collagen I (354236, Corning) at 5 μg/cm^2 in 0.02 N acetic acid (100063, Sigma-Aldrich) for one hour at room temperature. Wells were washed twice with PBS and dried at room temp. Epithelial cells were seeded at 14,000 cells/well. On day 3, cells were fixed in 4% PFA (28908, Thermo Fisher Scientific) for one hour at room temperature and the post-dewax steps of the immunofluorescence protocol above were followed.

qPCR
Total RNA was extracted using the Quick-RNA Miniprep Plus kit (Zymo Research) according to the manufacturer's instructions. cDNA was synthesised using qScript cDNA Supermix

(95048-100, Quantabio). Quantitative PCR was performed with SYBR Green (4367659, Thermo Fisher Scientific) using QuantStudio5™ Real-time PCR system (Thermo Fisher Scientific). A list of primers used for qPCR is provided in **Table S4**. Statistics were performed on dCt values. Relative gene expression was calculated using a comparative CT method with reference genes (*RPS13* and *GAPDH* for human genes, *Actb and/or Hprt1* for mouse genes).

In vivo experiment

Animal studies were approved by the University College London Biological Services Ethical Review Committee and licensed under UK Home Office regulations (project licence P36565407). Male mice on the C57Bl/6 background (11-13 weeks of age) were administered one dose of 1-azakenpaullone (3 mg/kg of body weight) or vehicle control (3% DMSO, 50% PEG300, 5% Tween80 and 42% PBS) by intraperitoneal injection. After 24 hours, mice were sacrificed by overdose of pentobarbital for isolation of tracheal and lung tissue. To determine cell proliferation, EdU (Merck) was administered with 1-azakenpaullone 24 hours before harvesting (15 mg/mL of EdU, 50 μg/g body weight), and alone two hours before harvesting (5 mg/ml of EdU, 50 μg/g body weight).

For qPCR analysis of tracheal epithelium, dissected trachea were first incubated in dispase (50 Unit/ml, 354235, Corning) for 40 minutes at 37°C. Following incubation, the epithelial layer was flushed from the trachea with 10 mL ice-cold PBS into a 15 mL tube using a needle and syringe. Cells were centrifuged at 400 x g and resuspended in RNA lysis buffer for RNA extraction.

To enable immunofluorescence staining of the tracheal epithelium, dissected tracheas were fixed in 4% PFA at 4°C overnight and then stored in 70% ethanol at 4°C before being processed in a Leica TP1050 tissue processor. Samples were embedded in type 6 paraffin wax (8336, Epredia) using an embedding station (Sakura Tissue-TEK TEC) and 5 μm sections were cut on a Microm HM 325 microtome.

To automate quantification analyses, macros were created in Fiji (Schindelin et al., 2012) to mask and quantify the count and area of immunofluorescent staining. Counts were performed on tracheal sections by two independent researchers blinded to the condition groups. The mean EdU proportion was taken per section.

Western blotting

Mouse lungs were snap frozen on dry ice, minced with a scalpel, homogenised and lysed in RIPA lysis buffer with protease inhibitors (cOmplete Ultra tablets, 5892970001, Merck) on ice to extract protein. 30 µg of protein samples were separated by SDS-PAGE and transferred onto nitrocellulose membranes using an iBlot2 Dry Blotting System (Thermo Fisher Scientific). Membranes were incubated with anti-cyclinD1 (55506, Cell Signaling Technologies), anti-c-myc (ab32072, Abcam), or anti-alpha-tubulin (9099, Cell Signaling Technologies) antibodies, washed, incubated with species-appropriate horseradish peroxidase (HRP)-conjugated secondary antibodies. After incubating with the substrate (Immobilon Crescendo Western HRP Substrate; WBLUR0500, Millipore), chemiluminescent signals were visualised using an iBright FL1500 imaging system (Thermo Fisher Scientific). Quantification of bands was performed using ImageJ (Image Processing and Analysis in Java, The National Institute of Health).

AUTHOR CONTRIBUTIONS

ACKNOWLEDGEMENTS

COMPETING INTERESTS

The S.M.J. has received fees for advisory board membership from BARD1 Life Sciences. S.M.J. has received grant income from GRAIL Inc. and is an unpaid member of a GRAIL advisory board. S.M.J. has received a lecture fee for an academic meeting from AstraZeneca. The remaining authors declare no competing or financial interests.

FUNDING

DATA AVAILABILITY

All relevant data can be found within the article and its supplemental information.

REFERENCES

Aros, C. J., Paul, M. K., Pantoja, C. J., Bisht, B., Meneses, L. K., Vijayaraj, P., Sandlin, J. M., France, B., Tse, J. A., Chen, M. W., et al. (2020a). High-Throughput Drug Screening Identifies a Potent Wnt Inhibitor that Promotes Airway Basal Stem Cell Homeostasis. *Cell Rep.* **30**, 2055–2064.e5.

Aros, C. J., Vijayaraj, P., Pantoja, C. J., Bisht, B., Meneses, L. K., Sandlin, J. M., Tse, J. A., Chen, M. W., Purkayastha, A., Shia, D. W., et al. (2020b). Distinct Spatiotemporally Dynamic Wnt-Secreting Niches Regulate Proximal Airway Regeneration and Aging. *Cell Stem Cell* **27**, 413–429.e4.

Ashburn, T. T. and Thor, K. B. (2004). Drug repositioning: identifying and developing new uses for existing drugs. *Nat. Rev. Drug Discov.* **3**, 673–683.

Baarsma, H. A., Skronska-Wasek, W., Mutze, K., Ciolek, F., Wagner, D. E., John-Schuster, G., Heinzelmann, K., Günther, A., Bracke, K. R., Dagouassat, M., et al. (2017). Noncanonical WNT-5A signaling impairs endogenous lung repair in COPD. *J. Exp. Med.* **214**, 143–163.

Basil, M. C., Katzen, J., Engler, A. E., Guo, M., Herriges, M. J., Kathiriya, J. J., Windmueller, R., Ysasi, A. B., Zacharias, W. J., Chapman, H. A., et al. (2020). The Cellular and Physiological Basis for Lung Repair and Regeneration: Past, Present, and Future. *Cell Stem Cell* **26**, 482–502.

Berdigaliyev, N. and Aljofan, M. (2020). An overview of drug discovery and development. *Future Med. Chem.* **12**, 939–947.

Bloom, B. (2021). Building the future of drug discovery. *Drug Discov. Today* **26**, 863–864.

Bustamante-Marin, X. M. and Ostrowski, L. E. (2017). Cilia and Mucociliary Clearance. *Cold Spring Harb. Perspect. Biol.* **9**,.

Butler, C. R., Hynds, R. E., Gowers, K. H. C., Lee, D. D. H., Brown, J. M., Crowley, C., Teixeira, V. H., Smith, C. M., Urbani, L., Hamilton, N. J., et al. (2016). Rapid Expansion of Human Epithelial Stem Cells Suitable for Airway Tissue Engineering. *Am. J. Respir. Crit. Care Med.* **194**, 156–168.

Cooney, R. A., Saal, M. L., Geraci, K. P., Maynard, C., Cleaver, O., Hoang, O. N., Moore, T. T., Hwang, R. F., Axelrod, J. D. and Vladar, E. K. (2023). A WNT4- and DKK3-driven canonical to noncanonical Wnt signaling switch controls multiciliogenesis. *J. Cell Sci.* **136**,.

Costa, R., Wagner, D. E., Doryab, A., De Santis, M. M., Schorpp, K., Rothenaigner, I., Lehmann, M., Baarsma, H. A., Liu, X., Schmid, O., et al. (2021). A drug screen with approved compounds identifies amlexanox as a novel Wnt/β-catenin activator inducing lung epithelial organoid formation. *Br. J. Pharmacol.* **178**, 4026–4041.

Danahay, H., Pessotti, A. D., Coote, J., Montgomery, B. E., Xia, D., Wilson, A., Yang, H., Wang, Z., Bevan, L., Thomas, C., et al. (2015). Notch2 is required for inflammatory cytokine-driven goblet cell metaplasia in the lung. *Cell Rep.* **10**, 239–252.

Feng, Z.-C., Donnelly, L., Li, J., Krishnamurthy, M., Riopel, M. and Wang, R. (2012). Inhibition of Gsk3β activity improves β-cell function in c-KitWv/+ male mice. *Lab. Invest.* **92**, 543–555.

Fulcher, M. L., Gabriel, S., Burns, K. A., Yankaskas, J. R. and Randell, S. H. (2005). Well-differentiated human airway epithelial cell cultures. *Methods Mol. Med.* **107**, 183–206.

Ghosh, M., Miller, Y. E., Nakachi, I., Kwon, J. B., Barón, A. E., Brantley, A. E., Merrick, D. T., Franklin, W. A., Keith, R. L. and Vandivier, R. W. (2018). Exhaustion of Airway Basal Progenitor Cells in Early and Established Chronic Obstructive Pulmonary Disease. *Am. J. Respir. Crit. Care Med.* **197**, 885–896.

Goss, A. M., Tian, Y., Tsukiyama, T., Cohen, E. D., Zhou, D., Lu, M. M., Yamaguchi, T. P. and Morrisey, E. E. (2009). Wnt2/2b and beta-catenin signaling are necessary and sufficient to specify lung progenitors in the foregut. *Dev. Cell* **17**, 290–298.

Haas, M., Gómez Vázquez, J. L., Sun, D. I., Tran, H. T., Brislinger, M., Tasca, A., Shomroni, O., Vleminckx, K. and Walentek, P. (2019). ΔN-Tp63 Mediates Wnt/β-Catenin-Induced Inhibition of Differentiation in Basal Stem Cells of Mucociliary Epithelia. *Cell Rep.* **28**, 3338–3352.e6.

Hashimoto, S., Chen, H., Que, J., Brockway, B. L., Drake, J. A., Snyder, J. C., Randell, S. H. and Stripp, B. R. (2012). β-Catenin-SOX2 signaling regulates the fate of developing airway epithelium. *J. Cell Sci.* **125**, 932–942.

Hiemstra, P. S., Grootaers, G., van der Does, A. M., Krul, C. A. M. and Kooter, I. M. (2018). Human lung epithelial cell cultures for analysis of inhaled toxicants: Lessons learned and future directions. *Toxicol. In Vitro* **47**, 137–146.

Horani, A., Nath, A., Wasserman, M. G., Huang, T. and Brody, S. L. (2013). Rho-associated protein kinase inhibition enhances airway epithelial Basal-cell proliferation and lentivirus transduction. *Am. J. Respir. Cell Mol. Biol.* **49**, 341–347.

Hsu, H.-S., Liu, C.-C., Lin, J.-H., Hsu, T.-W., Su, K. and Hung, S.-C. (2014). Repair of naphthalene-induced acute tracheal injury by basal cells depends on β-catenin. *J. Thorac. Cardiovasc. Surg.* **148**, 322–332.

Hynds, R. E. (2022). Exploiting the potential of lung stem cells to develop pro-regenerative therapies. *Biol. Open* **11**,.

Hynds, R. E., Gowers, K. H. C., Nigro, E., Butler, C. R., Bonfanti, P., Giangreco, A., Prêle, C. M. and Janes, S. M. (2018). Cross-talk between human airway epithelial cells and 3T3-J2 feeder cells involves partial activation of human MET by murine HGF. *PLoS One* **13**, e0197129.

Hynds, R. E., Butler, C. R., Janes, S. M. and Giangreco, A. (2019). Expansion of Human Airway Basal Stem Cells and Their Differentiation as 3D Tracheospheres. *Methods Mol. Biol.* **1576**, 43–53.

Ievlev, V., Jensen-Cody, C. C., Lynch, T. J., Pai, A. C., Park, S., Shahin, W., Wang, K., Parekh, K. R. and Engelhardt, J. F. (2022). Sox9 and Lef1 Regulate the Fate and Behavior of Airway Glandular Progenitors in Response to Injury. *Stem Cells* **40**, 778–790.

Iversen, P. W., Beck, B., Chen, Y.-F., Dere, W., Devanarayan, V., Eastwood, B. J., Farmen, M. W., Iturria, S. J., Montrose, C., Moore, R. A., et al. (2012). HTS Assay Validation. In *Assay Guidance Manual* (ed. Markossian, S.), Grossman, A.), Arkin, M.), Auld, D.), Austin, C.), Baell, J.), Brimacombe, K.), Chung, T. D. Y.), Coussens, N. P.), Dahlin, J. L.), et al.), Bethesda (MD): Eli Lilly & Company and the National Center for

Advancing Translational Sciences.

Johnson, J. E., Gonzales, R. A., Olson, S. J., Wright, P. F. and Graham, B. S. (2007). The histopathology of fatal untreated human respiratory syncytial virus infection. *Mod. Pathol.* **20**, 108–119.

Kassis, T., Hernandez-Gordillo, V., Langer, R. and Griffith, L. G. (2019). OrgaQuant: Human Intestinal Organoid Localization and Quantification Using Deep Convolutional Neural Networks. *Sci. Rep.* **9**, 12479.

Kicic, A., Hallstrand, T. S., Sutanto, E. N., Stevens, P. T., Kobor, M. S., Taplin, C., Paré, P. D., Beyer, R. P., Stick, S. M. and Knight, D. A. (2010). Decreased fibronectin production significantly contributes to dysregulated repair of asthmatic epithelium. *Am. J. Respir. Crit. Care Med.* **181**, 889–898.

Kunick, C., Lauenroth, K., Leost, M., Meijer, L. and Lemcke, T. (2004). 1-Azakenpaullone is a selective inhibitor of glycogen synthase kinase-3 beta. *Bioorg. Med. Chem. Lett.* **14**, 413–416.

Lau, C. H., Rouhani, M. J., Maughan, E. F., Orr, J. C., Kolluri, K. K., Pearce, D. R., Haughey, E. K., Sutton, L., Flatau, S., Balboa, P. L., et al. (2024). Lentiviral expression of wild-type LAMA3A restores cell adhesion in airway basal cells from children with epidermolysis bullosa. *Mol. Ther.*

Lee, D. D. H., Cardinale, D., Nigro, E., Butler, C. R., Rutman, A., Fassad, M. R., Hirst, R. A., Moulding, D., Agrotis, A., Forsythe, E., et al. (2021). Higher throughput drug screening for rare respiratory diseases: readthrough therapy in primary ciliary dyskinesia. *Eur. Respir. J.* **58**,.

Leost, M., Schultz, C., Link, A., Wu, Y.-Z., Biernat, J., Mandelkow, E.-M., Bibb, J. A., Snyder, G. L., Greengard, P., Zaharevitz, D. W., et al. (2000). Paullones are potent inhibitors of glycogen synthase kinase-3β and cyclin-dependent kinase 5/p25. *Eur. J. Biochem.* **267**, 5983–5994.

Li, C., Li, A., Li, M., Xing, Y., Chen, H., Hu, L., Tiozzo, C., Anderson, S., Taketo, M. M. and Minoo, P. (2009). Stabilized beta-catenin in lung epithelial cells changes cell fate and leads to tracheal and bronchial polyposis. *Dev. Biol.* **334**, 97–108.

Liu, X., Ory, V., Chapman, S., Yuan, H., Albanese, C., Kallakury, B., Timofeeva, O. A., Nealon, C., Dakic, A., Simic, V., et al. (2012). ROCK inhibitor and feeder cells induce the conditional reprogramming of epithelial cells. *Am. J. Pathol.* **180**, 599–607.

Lynch, T. J., Anderson, P. J., Xie, W., Crooke, A. K., Liu, X., Tyler, S. R., Luo, M., Kusner, D. M., Zhang, Y., Neff, T., et al. (2016). Wnt Signaling Regulates Airway Epithelial Stem Cells in Adult Murine Submucosal Glands. *Stem Cells* **34**, 2758–2771.

Malleske, D. T., Hayes, D., Jr, Lallier, S. W., Hill, C. L. and Reynolds, S. D. (2018). Regulation of Human Airway Epithelial Tissue Stem Cell Differentiation by β-Catenin, P300, and CBP. *Stem Cells* **36**, 1905–1916.

Mayr, L. M. and Bojanic, D. (2009). Novel trends in high-throughput screening. *Curr. Opin. Pharmacol.* **9**, 580–588.

Meijer, L., Skaltsounis, A.-L., Magiatis, P., Polychronopoulos, P., Knockaert, M., Leost, M., Ryan, X. P., Vonica, C. A., Brivanlou, A., Dajani, R., et al. (2003). GSK-3-selective inhibitors derived from Tyrian purple indirubins. *Chem. Biol.* **10**, 1255–1266.

Nizamoglu, M., Joglekar, M. M., Almeida, C. R., Larsson Callerfelt, A.-K., Dupin, I., Guenat, O. T., Henrot, P., van Os, L., Otero, J., Elowsson, L., et al. (2023). Innovative three-dimensional models for understanding mechanisms underlying lung diseases: powerful tools for translational research. *Eur. Respir. Rev.* **32**,.

O'Koren, E. G., Hogan, B. L. M. and Gunn, M. D. (2013). Loss of basal cells precedes bronchiolitis obliterans-like pathological changes in a murine model of chlorine gas inhalation. *Am. J. Respir. Cell Mol. Biol.* **49**, 788–797.

Orellana, A., García-González, V., López, R., Pascual-Guiral, S., Lozoya, E., Díaz, J., Casals, D., Barrena, A., Paris, S., Andrés, M., et al. (2018). Application of a phenotypic drug discovery strategy to identify biological and chemical starting points for inhibition of TSLP production in lung epithelial cells. *PLoS One* **13**, e0189247.

Orr, J. C. and Hynds, R. E. (2021). Stem Cell-derived Respiratory Epithelial Cell Cultures as Human Disease Models. *Am. J. Respir. Cell Mol. Biol.* **64**, 657–668.

Pushpakom, S., Iorio, F., Eyers, P. A., Escott, K. J., Hopper, S., Wells, A., Doig, A., Guilliams, T., Latimer, J., McNamee, C., et al. (2019). Drug repurposing: progress, challenges and recommendations. *Nat. Rev. Drug Discov.* **18**, 41–58.

Reynolds, S. D., Rios, C., Wesolowska-Andersen, A., Zhuang, Y., Pinter, M., Happoldt, C., Hill, C. L., Lallier, S. W., Cosgrove, G. P., Solomon, G. M., et al. (2016). Airway Progenitor Clone Formation Is Enhanced by Y-27632-Dependent Changes in the Transcriptome. *Am. J. Respir. Cell Mol. Biol.* **55**, 323–336.

Rim, E. Y., Clevers, H. and Nusse, R. (2022). The Wnt Pathway: From Signaling Mechanisms to Synthetic Modulators. *Annu. Rev. Biochem.* **91**, 571–598.

Rock, J. R., Onaitis, M. W., Rawlins, E. L., Lu, Y., Clark, C. P., Xue, Y., Randell, S. H. and Hogan, B. L. M. (2009). Basal cells as stem cells of the mouse trachea and human airway epithelium. *Proc. Natl. Acad. Sci. U. S. A.* **106**, 12771–12775.

Schindelin, J., Arganda-Carreras, I., Frise, E., Kaynig, V., Longair, M., Pietzsch, T., Preibisch, S., Rueden, C., Saalfeld, S., Schmid, B., et al. (2012). Fiji: an open-source platform for biological-image analysis. *Nat. Methods* **9**, 676–682.

Schmid, A., Sailland, J., Novak, L., Baumlin, N., Fregien, N. and Salathe, M. (2017). Modulation of Wnt signaling is essential for the differentiation of ciliated epithelial cells in human airways. *FEBS Lett.* **591**, 3493–3506.

Sen, C., Rickabaugh, T. M., Jeyachandran, A. V., Yuen, C., Ghannam, M., Durra, A., Aziz, A., Castillo, K., Garcia, G., Jr, Purkayastha, A., et al. (2024). High throughput screening with a primary human mucociliary airway model identifies a small molecule with anti-SARS-CoV-2 activity. *bioRxiv*.

Shu, W., Guttentag, S., Wang, Z., Andl, T., Ballard, P., Lu, M. M., Piccolo, S., Birchmeier, W., Whitsett, J. A., Millar, S. E., et al. (2005). Wnt/beta-catenin signaling acts upstream of N-myc, BMP4, and FGF signaling to regulate proximal-distal patterning in the lung. *Dev. Biol.* **283**, 226–239.

Staudt, M. R., Buro-Auriemma, L. J., Walters, M. S., Salit, J., Vincent, T., Shaykhiev, R., Mezey, J. G., Tilley, A. E., Kaner, R. J., Ho, M. W. Y., et al. (2014). Airway Basal stem/progenitor cells have diminished capacity to regenerate airway epithelium in chronic obstructive pulmonary disease. *Am. J. Respir. Crit. Care Med.* **190**, 955–958.

Stevens, P. T., Kicic, A., Sutanto, E. N., Knight, D. A. and Stick, S. M. (2008). Dysregulated repair in asthmatic paediatric airway epithelial cells: the role of plasminogen activator inhibitor-1. *Clin. Exp. Allergy* **38**, 1901–1910.

Sun, D., Gao, W., Hu, H. and Zhou, S. (2022). Why 90% of clinical drug development fails and how to improve it? *Acta Pharm Sin B* **12**, 3049–3062.

Tadokoro, T., Wang, Y., Barak, L. S., Bai, Y., Randell, S. H. and Hogan, B. L. M. (2014). IL-6/STAT3 promotes regeneration of airway ciliated cells from basal stem cells. *Proc. Natl. Acad. Sci. U. S. A.* **111**, E3641–9.

Taubenberger, J. K. and Morens, D. M. (2008). The pathology of influenza virus infections. *Annu. Rev. Pathol.* **3**, 499–522.

Turner, R. B., Hendley, J. O. and Gwaltney, J. M., Jr (1982). Shedding of infected ciliated epithelial cells in rhinovirus colds. *J. Infect. Dis.* **145**, 849–853.

Walsh, J. J., Dietlein, L. F., Low, F. N., Burch, G. E. and Mogabgab, W. J. (1961). Bronchotracheal response in human influenza. Type A, Asian strain, as studied by light and electron microscopic examination of bronchoscopic biopsies. *Arch. Intern. Med.* **108**, 376–388.

Warner, S. M. B., Hackett, T.-L., Shaheen, F., Hallstrand, T. S., Kicic, A., Stick, S. M. and Knight, D. A. (2013). Transcription factor p63 regulates key genes and wound repair in human airway epithelial basal cells. *Am. J. Respir. Cell Mol. Biol.* **49**, 978–988.

Wijk, S. C., Prabhala, P., Michaliková, B., Sommarin, M., Doyle, A., Lang, S., Kanzenbach, K., Tufvesson, E., Lindstedt, S., Leigh, N. D., et al. (2021). Human Primary Airway Basal Cells Display a Continuum of Molecular Phases from Health to Disease in Chronic Obstructive Pulmonary Disease. *Am. J. Respir. Cell Mol. Biol.* **65**, 103–113.

Zaharevitz, D. W., Gussio, R., Leost, M., Senderowicz, A. M., Lahusen, T., Kunick, C., Meijer, L. and Sausville, E. A. (1999). Discovery and initial characterization of the paullones, a novel class of small-molecule inhibitors of cyclin-dependent kinases. *Cancer Res.* **59**, 2566–2569.

Zhang, Y., Black, K. E., Phung, T.-K. N., Thundivalappil, S. R., Lin, T., Wang, W., Xu, J., Zhang, C., Hariri, L. P., Lapey, A., et al. (2023). Human Airway Basal Cells Undergo Reversible Squamous Differentiation and Reshape Innate Immunity. *Am. J. Respir. Cell Mol. Biol.* **68**, 664–678.
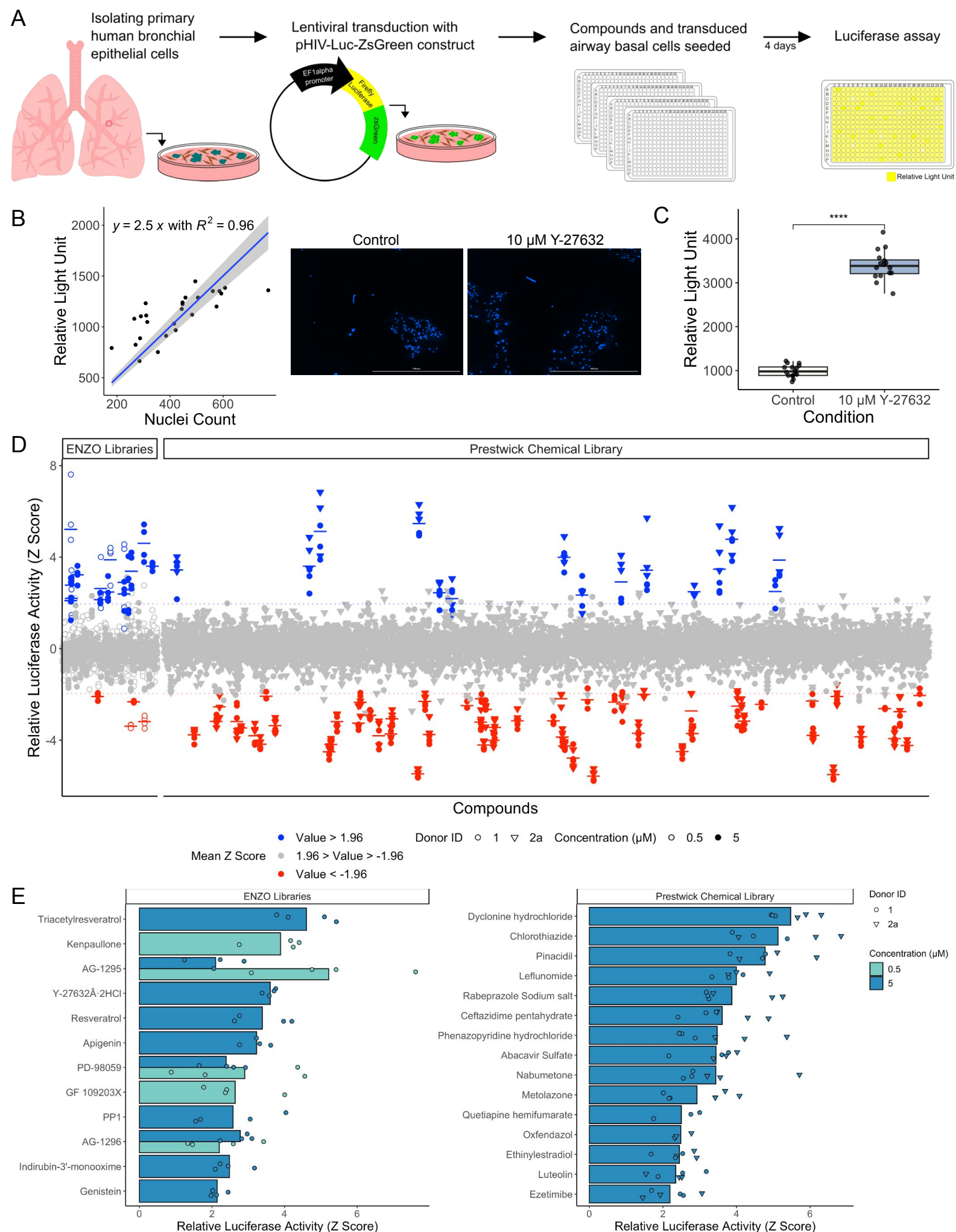
Figure 1: High-throughput screening of 1,429 compounds identifies compounds that modulate airway basal cell proliferation.

A) Schematic representation of the 384-well format screening approach. Primary human airway basal cells were transduced with a pHIV-Luc-zsGreen lentivirus to enable luciferase monitoring of cell proliferation. Cells were seeded in 384-well format and treated with compounds from the ENZO chemical library and the Prestwick Chemical library for four days before luciferin was added to the culture medium and bioluminescence was measured.

B) Correlation between bioluminescence and nuclei count (left; n = 16 wells, donor ID 1, see also Supplemental Fig. 1D). Representative images of Hoechst 33342 staining of cells following the luciferase assay (right). Scale bars = 1,000 μm.

C) Bioluminescence readings in the 384-well format assay comparing control or 10 μM Y-27632 treated wells (n = 16 wells, donor ID 1, Wilcoxon test, ****=p<0.0001).

D) 1429 compounds from either an epigenetic modulator, protease and kinase inhibitor library (ENZO Life Sciences) or the Prestwick Chemical library were screened in transduced airway basal cells (n = 2 donors [ID 1 = circles, ID 2 = triangles]) in triplicate. Z Scores were calculated from the relative light unit values. Hit compounds (blue) were identified as those with a mean Z Score above 1.96 standard deviations of the plate average (above the grey dotted line). Red colour indicates compounds with a mean Z Score below 1.96 standard deviations of the plate average.

E) Hit compounds identified from screening of the ENZO chemical library (left) and the Prestwick Chemical library (right) [donor ID1 = circles, ID2a = triangles].
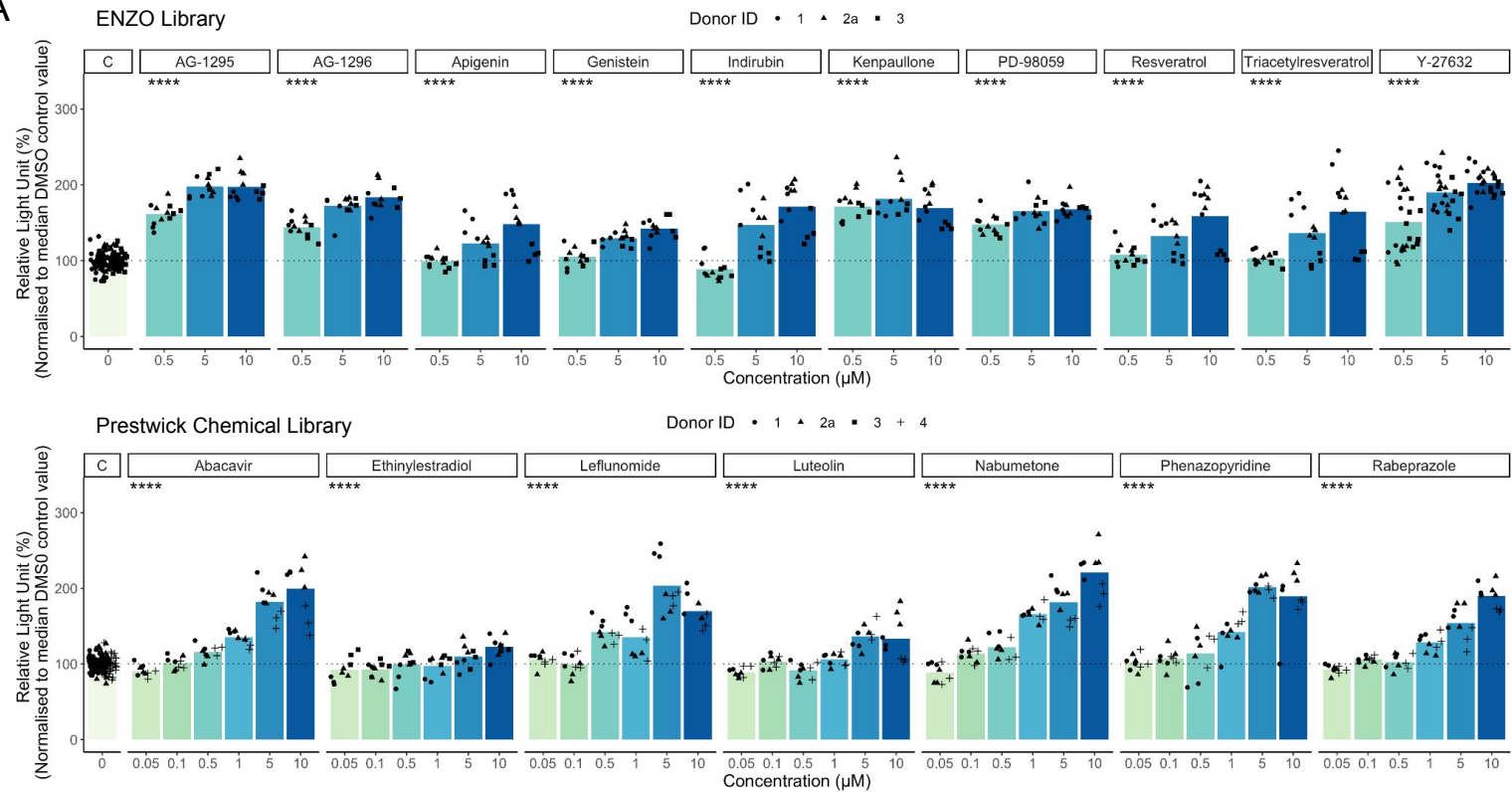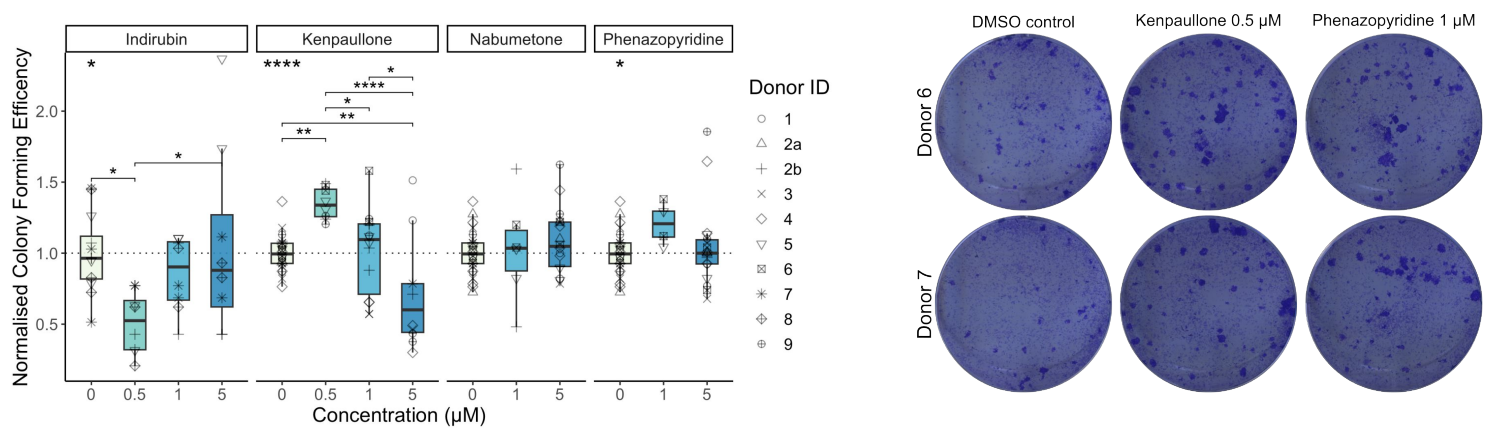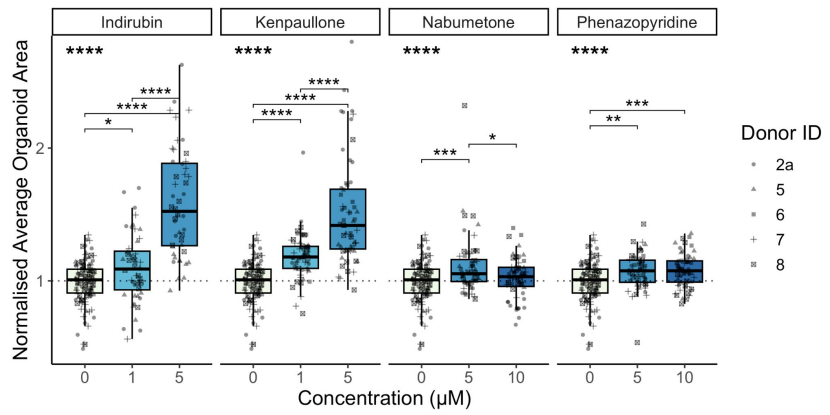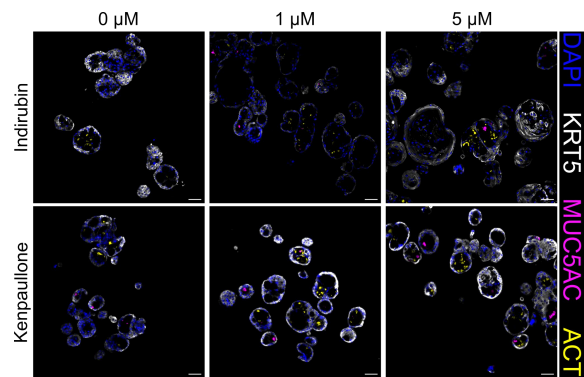
Figure 2: Validation of pro-proliferative compounds in 2D and 3D primary cell culture models.

A) Four-day concentration-response proliferation assays in primary human airway basal cells transduced with the pHIV-Luc-zsGreen construct for compounds identified within the ENZO chemical library (upper panel) or the Prestwick Chemical library (lower panel; n = 3 donors per compound; donor ID1 = circles, ID2a = triangles, ID3 = squares, ID4 = cross). An ANOVA was performed per compound, **** = $p<0.0001$.

B) Quantification of airway basal cell colony formation efficiency for four validated hit compounds identified as Wnt activating molecules (left; n=3-9 donors per compound) and representative well images from the 0.5 µM kenpaullone - and 1 µM phenazopyridine-treated wells (right). An ANOVA was performed per compound and significant Tukey's HSD values are shown. * = $p<0.05$, ** = $p<0.01$, **** = $p<0.0001$.

C) Quantification of mean organoid size per well with 12 replicate wells per condition were normalised to mean control well organoid size for each donor (n = 4/5 donors per compound; donor ID1 = circles, ID2a = triangles, ID3 = squares, ID4 = cross). An ANOVA was performed per compound and significant Tukey's HSD values are shown. * = $p<0.05$, ** = $p<0.01$, ***= $p<0.001$, **** = $p<0.0001$). Control well data are repeated per compound facet.

D) Representative immunofluorescence staining of organoids cultured in the presence of indirubin-3'-monoxime or kenpaullone (n=5, donor ID= 8 shown). Staining for keratin 5 (KRT5; basal cells, white), MUC5AC (mucosecretory cells, magenta) and ACT (multiciliated cells, yellow). Scale bars = 50 µm.
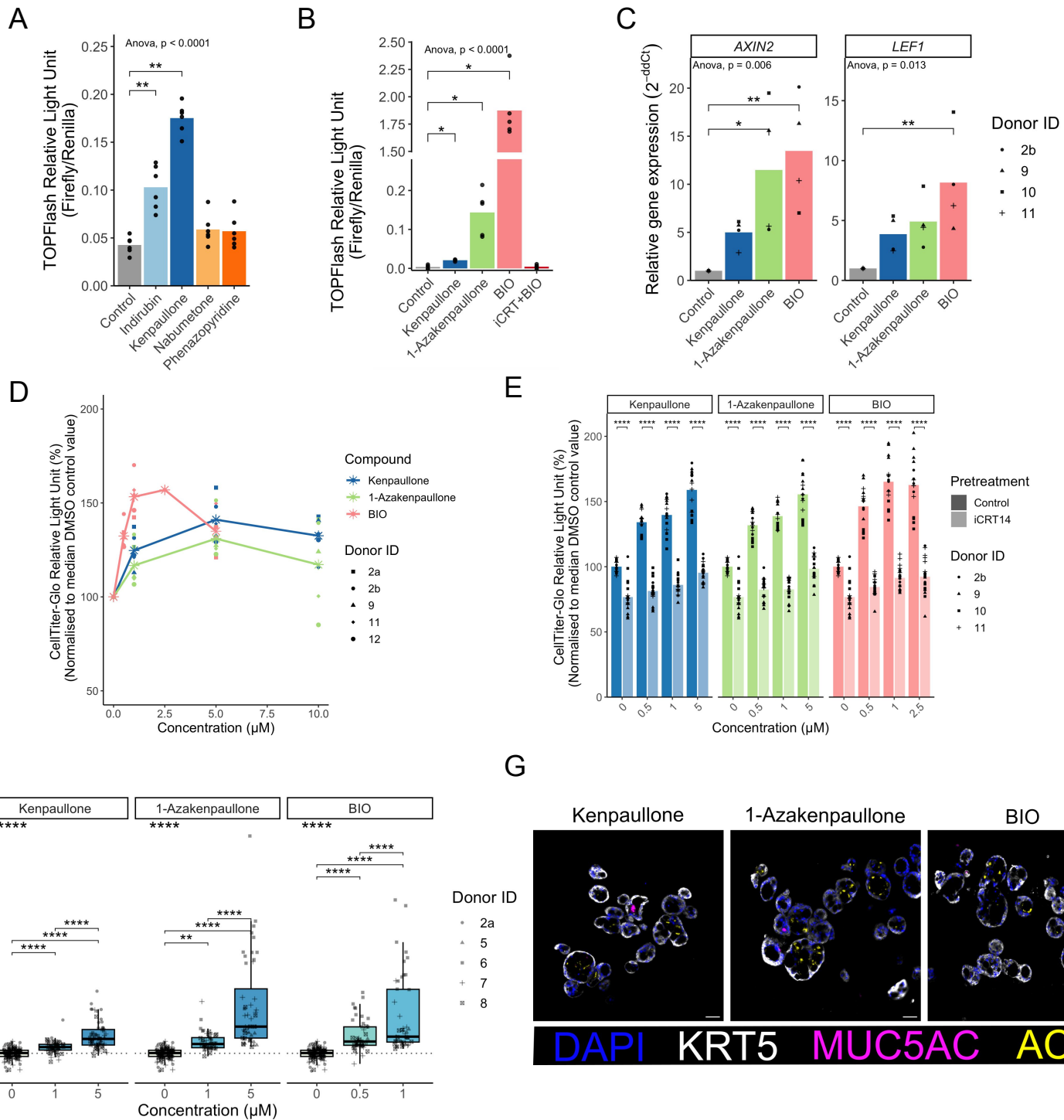
Figure 3: Investigation of Wnt pathway activating compounds as promoters of airway basal cell proliferation.

A) Quantification of Wnt activity using the TOPFlash assay. HBEC3-KT cells were transfected with TOPFlash plasmid, re-plated in a 384-well plate and incubated with 10 µM of the indicated compounds for 24 hours. An ANOVA was performed and a Wilcoxon t-test with Holm correction for multiple testing to compare control and compound treated wells. ** = $p<0.01$.

B) Quantification of Wnt activity using the TOPFlash assay in HBEC3-KT cells treated with kenpaullone, 1-azakenpaullone, BIO, or BIO and iCRT14 (a Wnt pathway inhibitor) for 24 hours. Negative control FOPFlash assays performed in parallel were negative as expected (not shown). An ANOVA was performed and a Wilcoxon t-test with Holm correction for multiple testing to compare control and compound treated wells. * = $p<0.05$.

C) qPCR analysis of the Wnt target genes *LEF1* and *AXIN2*. Primary human airway basal cells (n = 4 donors) were treated with compounds for 24 hours. Relative expression was determined by normalising to the reference genes *RPS13* and *GAPDH*. An ANOVA test was performed per target gene and significant Tukey's HSD values are shown.

D) Quantification of primary human airway basal cell proliferation over six days using the CellTiter-Glo assay. Data are normalised to control wells containing the highest concentration of DMSO used in the experimental conditions. Points are the mean value of quadruplicate wells per donor (n = 5 donors).

E) Effect of the Wnt pathway inhibitor iCRT14 on the proliferation of airway basal cells in the presence of kenpaullone, 1-azakenpaullone or BIO. Cells were pre-treated with 10 µM iCRT14 or DMSO control for 24 hours before the addition of the Wnt activating compounds. Relative growth was assessed after two days using the CellTiter-Glo assay (n = 4 donors). Wilcoxon tests were performed with Holm correction for multiple testing per compound, ****$p<0.0001$.

F) Quantification of mean organoid size per well with 12 replicate wells per condition were normalised to mean control well organoid size for each donor (n = 5 donors [ID2a = circles, ID5 = triangles, ID6 = squares, ID7 = cross, ID8 = checked box]. An ANOVA was performed per compound and significant Tukey's HSD values are shown. ** = $p<0.01$, **** = $p<0.0001$). Control well data are repeated per compound facet and kenpaullone data is repeated from Figure 2C.

G) Immunofluorescence staining showing KRT5 (basal cells, white), MUC5AC (mucosecretory cells, magenta), and ACT (ciliated cells, yellow) in organoids following culture in medium containing the indicated compounds (n=5, donor ID= 8 shown). Scale bars = 50 µm.
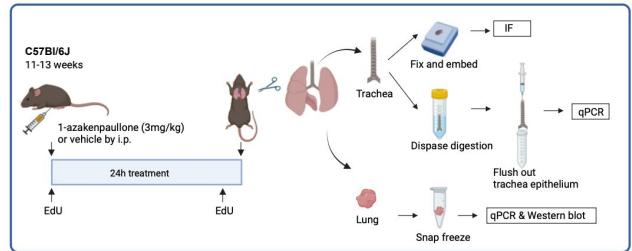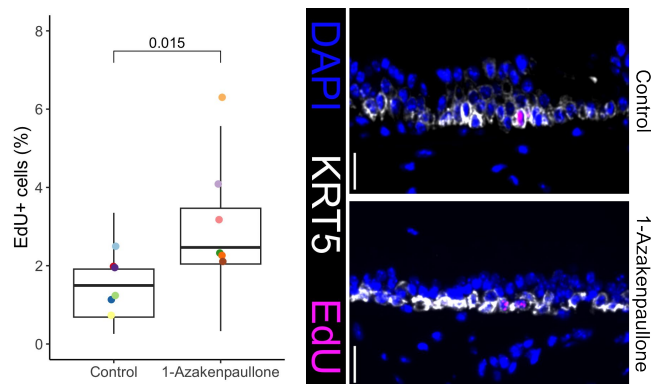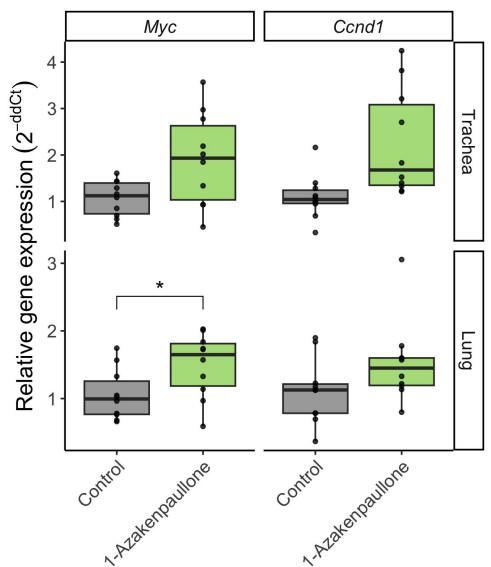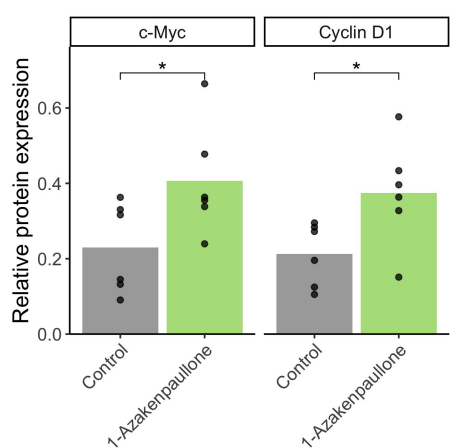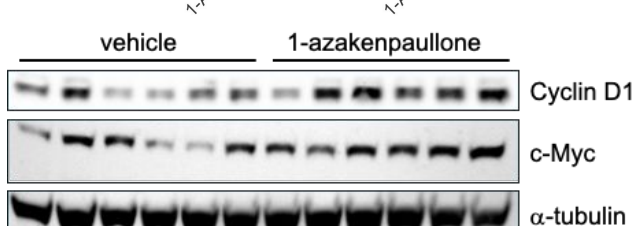
Figure 4: 1-Azakenpaullone induced tracheal proliferation and the expression of Wnt target genes *in vivo*.

A) Schematic representation of the *in vivo* experimental design. Male C57Bl/6 mice (n = 10 in each group) were administered EdU, and 1-azakenpaullone (3 mg/kg body weight) or vehicle control by intraperitoneal injection. After 24 hours, mice were sacrificed and tracheas and lungs were harvested for analysis.

B) Quantification of tracheal proliferation by EdU staining in mice treated with 1-azakenpaullone (3 mg/kg body weight) or vehicle control (n = 6 mice/condition; left). Points indicate mean values per mouse and boxplot represents data from individual images. Wilcoxon test p value shown. Immunofluorescence staining showing KRT5 (basal cells, white) and EdU (magenta) om mouse tracheal sections (right). Scale bars= 20 µm.

C) Expression of the Wnt target genes *Myc and Ccnd1* in mouse trachea or and lung as determined by qPCR. Relative expression was normalised to *HPRT1* and/or *ACTB.* A Wilcoxon test was performed (n = 10 mice per group, * p < 0.05).

D) Expression of Wnt target proteins in lung tissue as determined by Western blot (n = 6 per group). Alpha-tubulin is shown as a loading control. The bands were quantified using ImageJ and the relative expression of c-Myc and CyclinD1 normalised to alpha-tubulin are shown. A Wilcoxon test was performed, * p < 0.05.